Proc. Estonian Acad. Sci. Phys. Math., 2005, **54**, 2, 98–110
https://doi.org/10.3176/phys.math.2005.2.04

Two-component scenario, cuprate related gaps, and superconducting density

Nikolai Kristoffel[a,b] and Pavel Rubin[b]

[a] Institute of Physics, University of Tartu, Riia 142, 51014 Tartu, Estonia; kolja@fi.tartu.ee
[b] Institute of Theoretical Physics, University of Tartu, Tähe 4, 51010 Tartu, Estonia

Received 12 November 2004, in revised form 24 January 2005

Abstract. A simple model of cuprate superconductivity with an electron spectrum prepared by doping is developed. The pair-transfer interaction couples the itinerant band with two components ("hot" and "cold") of the defect subsystem. Basic defect-itinerant gaps are quenched by progressive doping. Band overlaps appear as novel sources for critical doping concentrations. Insulator to metal transitions in the normal state are expected here. Minimal quasiparticle excitation energies determine the pseudo- and superconducting gaps according to the doping-dependent disposition of bands. Two pseudogaps can be present at underdoping and two superconducting gaps can be manifested at overdoping. Various transformations and connections between the gaps, pseudogaps, and normal state gaps agree with various experimental findings. The superconducting density does not reflect the presence of "extrinsic" gaps because of the interband nature of the pairing. A Uemura-type sublinear plot at underdoping with further recession is obtained. A mixed Fermi-liquid is restored near optimal doping where the chemical potential intersects all the band components.

Key words: cuprate superconductivity, two-band model, doping, gaps, superfluid density.

1. INTRODUCTION

Extensive experimental data on superconductivity energetic characteristics have been collected for cuprates [1−14]. However, standardized measurements covering self-consistently and smoothly the whole energy and doping scales are advisable. The presence of at least one superconducting gap and one or even two pseudogaps [4−7] raises a question about the number of superconductivity order parameters. Indications of the appearance of two superconducting gaps can be found. The nature of the pseudogap which survives in the normal state has still remained debatable [15]. "Extrinsic" and "intrinsic" mechanisms have

been proposed. In the latter case the pseudogap is caused by the fluctuating superconductivity order (preformed pairs) at $T > T_{\rm c}$ and an immediate connection exists between the superconducting gap and the pseudogap. The extrinsic mechanism looks for the pseudogap source in the normal state electron spectrum. Bare gaps in it may be due to other types of orderings (in the lattice–phonon subsystem) or doping. At present this kind of explanation seems to be preferable [2,11].

A cuprate superconductor can be considered as a charge-transfer insulator perturbed by doping. In what follows the excitations in the charge channel will be considered. The excitations in the spin-subsystem build up an essential associated partner. Controversial statements on interrelations of cuprate gaps have been made. These concern transformations of superconducting gaps into pseudogaps on doping, the connection of superconducting and normal state gaps, and the coexistence of various gaps in distinct doping regions.

We believe that one way to reach a more physical insight into cuprate superconducting properties on the excitation–energy–doping phase diagram will be the elaboration of a simple (possibly partly postulative) model by using the general knowledge of these systems. The following comparison of the qualitative outcome with observations can then illuminate the background physics.

Cuprate superconductivity is widely discussed in the two-component scenario [16,17]. Its essence consists in the statement that a "defect-polaronic" subsystem bearing doped holes is functioning besides the itinerant valence band electrons. The framework of the two-component scenario leaves freedom for the precision of the nature of the electronic background and pairing channels. One can, e.g., consider as basic ingredients a mainly oxygen band between the Cu-dominated Hubbard components and a distribution of states created by doping [7,13,18–23] near the top of this band. Lattice effects enter this scenario through the inhomogeneous structure of CuO_2 planes in doped cuprates (stripes, tweed patterns, granularity) and the associated electronic phase separation [17,24–27].

Attempts to reflect the two-component scenario by a simple model have been started in [18,19,28–30]. The present contribution is a generalization, especially concerning the superfluid density. Our model uses a nonrigid electronic playground of superconductivity prepared by doping. The "extrinsic" source of the pseudogaps lies in the postulated bare normal state gaps between the defect and the itinerant states. These will be quenched with progressive doping. The mutual transformations between superconducting gaps and pseudogaps can be explained by the change of the nature of the minimal quasiparticle excitation energy on doping. Correspondingly the pseudogap(s) appears as a gap in the quasiparticle spectrum. It does not follow the superconducting order parameters and does not compete with them. The connection between pseudogaps and normal state gaps is due to the mixing of the normal state spectrum with the superconducting gaps in the quasiparticle energy expression. The fluctuation effects have not been taken into account in this model (cf. [15]).

The electron spectrum considered in the two-component scenario is nonrigid. The appearance of a "defect" subsystem besides the itinerant one opens a novel channel for reaching high $T_{\rm c}$'s by the interband pair transfer interaction [19,20]. The corresponding two-band superconductivity mechanism [31,32] has been known for a long time. A number of attempts [33] have been made to use it for cuprates in connection with the two-component scenario [18,19,26,28−30,34−39]. The interband pairing interaction operates in a considerable volume of the momentum space and works for pairing also as being repulsive. It also prevents the manifestation of normal state gaps in the superfluid density (order parameters) [18,19].

2. THE MODEL

Various data exploited for the choice of the model are presented in [18,19,28−30]. A cuprate electron spectrum created and reorganized by doping is described as follows. The itinerant (valence) band (γ) states are lying between the energies $\xi = -D$ and $\xi(\max) = 0$ and are normalized to $1 - c$. Here c is a measure of the doped hole concentration. It must be scaled for a given case, e.g., by joining characteristic concentrations on the phase diagram.

The defect subsystem is structurally anisotropic, and this is manifested in different gap features over the momentum space [1−3,13,40]. The presence of two pseudogaps [5−7] of different behaviour is impressive. The well-expressed large pseudogap is connected with the neighbourhood of the "hot" $(\pi, 0)$-type Brillouin zone points. The spectrum at $(\frac{\pi}{2}, \frac{\pi}{2})$-type "cold" points seems to be weakly gapped [40]. For these reasons the defect system will be characterized by two subbands for the "hot" (α) and "cold" (β) regions (cf. [36]). These subbands occupy the energy intervals $d_1 - \alpha c$ and $d_2 - \beta c$, respectively, with the weight of states $c/2$ (cf. [23]). At underdoping these bands lie above the valence band. Note that the optical charge-transfer gap is reduced by doping [41]. A progressive doping brings first the β-band to overlap with the γ-band at $c_\beta = d_2\beta^{-1}$. A common overlapping distribution of all the bands starts at $c_\alpha = d_1\alpha^{-1}$. It is known that the infrared manifestation of the defect band is lost at larger dopings in favour of a Drude peak of (free) carriers [42].

The 2D (CuO_2 planes) densities of states of these bands read: $\rho_\gamma = (1-c)D^{-1}$, $\rho_\alpha = (2\alpha)^{-1}$, $\rho_\beta = (2\beta)^{-1}$, and $\beta < \alpha$ is supposed. There are three qualitatively different arrangements of the bands and the chemical potential (μ). At $c < c_\beta$, $\mu = d_2 - \beta c$ remains connected with the "cold" β-band. At underdoping the charge carriers are concentrated in this "cold" subsystem in accordance with [13]. For $c > c_\beta$, $\mu = (d_2 - \beta c)[1 + 2\beta(1 - c)D^{-1}]^{-1}$ intersects both (β, γ)-bands. For the expressed dopings larger than c_0, determined by $d_1 - \alpha c_0 = \mu$, the role of the $(\pi, 0)$-type region increases essentially (cf. [43,44]). Now the chemical potential $\mu = [\alpha d_2 + \beta d_1 - 2\alpha\beta c][\alpha + \beta + (1 - c)2\alpha\beta D^{-1}]^{-1}$ intersects all the three overlapping bands.

The valence band is attributed to the hole-poor regions of the material. It remains the source of antiferromagnetic fluctuations whereas in the defect space

distinct spin-structures can be built up (ferrons, polaron aggregates, etc.). This type of background has been used to describe the underdoped cuprate magnetic properties [37] and a bridge for explaining the presence of a magnetic pseudogap in the spin excitation channel opens.

There are also approaches to cuprate superconductivity based on the special role of the van Hove singularity peak in the CuO_2 (nondoped) plane spectrum [45]. The constant densities of states used in the present work for the doped spectrum are crude approximations. However, our joint active spectrum is to some extent analogous to [44]. The present model takes special account of the strongly perturbed region near the top of the itinerant band where also the Fermi level is positioned. The main point is the defect β-band creation. The relatively large and narrow density of states of this band shifts to the γ-band top and the whole spectrum resembles one supposed in "van Hove-type" scenarios. The interband pairing channel of the present model works effectively on this background of doping-driven spectral overlap resonance. Presumably the defect part of the spectrum can be compared with the bosonic (bipolaronic) component of the theories including bosonization [37,38].

3. BASIC EXPRESSIONS

The cuprate pairing mechanism will be described by the coupling of itinerant and defect subsystems through the pair-transfer [33] interaction. Superconductivity is mutually induced in interacting components. The corresponding coupling constant W contains Coulombic and electron-phonon (repulsive) contributions [33]. Pairs are formed from the particles of the same band.

The intraband contributions [33] are of less significance on the present level of the model. The basic mean field Hamiltonian reads

$$H = \sum_{\sigma,\vec{k},s} \epsilon(\vec{k}) a^{+}_{\sigma\vec{k}s} a_{\sigma\vec{k}s} + \sum_{\vec{k}} \Delta_{\gamma}(\vec{k}) [a_{\gamma\vec{k}\uparrow} a_{\gamma-\vec{k}\downarrow} + a^{+}_{\gamma-\vec{k}\downarrow} a^{+}_{\gamma\vec{k}\uparrow} - \sum_{\vec{k},\tau}{}^{\tau} \Delta_{\tau}(\vec{k}) [a_{\tau\vec{k}\uparrow} a_{\tau-\vec{k}\downarrow} + a^{+}_{\tau-\vec{k}\downarrow} a^{+}_{\tau\vec{k}\uparrow}]. \qquad (1)$$

Here $\epsilon_{\sigma} = \xi_{\sigma} - \mu$; $\sigma = \alpha, \beta, \gamma$; $\tau = \alpha, \beta$, and $\sum^{\tau}$ means the integration with the densities of states $\rho_{\alpha,\beta}$ in the corresponding energy intervals. Usual designations are applicable for spins (s) and electron operators. The superconductivity order parameters are defined as

$$\begin{aligned} \Delta_{\gamma}(\vec{q}) &= 2 \sum_{\vec{k},\tau}{}^{\tau} W(\vec{q},\vec{k}) < a_{\tau\vec{k}\uparrow} a_{\tau-\vec{k}\downarrow} >, \\ \Delta_{\tau}(\vec{q}) &= 2 \sum_{\vec{k}} W(\vec{q},\vec{k}) < a_{\gamma-\vec{k}\downarrow} a_{\gamma\vec{k}\uparrow} > . \end{aligned} \qquad (2)$$

The diagonalization of (1) yields the gap equation ($\Theta = k_B T$) system

$$\begin{aligned} \Delta_\gamma(\vec{q}) &= \sum_{\vec{k},\tau} {}^{\tau}W(\vec{q},\vec{k})\Delta_\tau(\vec{k})E_\tau^{-1}(\vec{k})th\frac{E_\tau(\vec{k})}{2\Theta}, \\ \Delta_\tau(\vec{q}) &= \sum_{\vec{k}} W(\vec{q},\vec{k})\Delta_\gamma(\vec{k})E_\gamma^{-1}(\vec{k})th\frac{E_\gamma(\vec{k})}{2\Theta}, \end{aligned} \tag{3}$$

with the usual form of the quasiparticle energies

$$E_\sigma(\vec{k}) = \sqrt{\epsilon_\sigma^2(\vec{k}) + \Delta_\sigma^2(\vec{k})}\ . \tag{4}$$

In what follows W will be taken as constant for simplicity. Moreover, $\Delta_\alpha = \Delta_\beta$ is set. At T_c, according to (3) the gaps Δ_σ tend simultaneously to zero. For $W > 0$ two s-type order parameters appear with the opposite signs [33]; Eq. (1) uses positive Δ values.

The density of paired carriers can be calculated as

$$n_s = \frac{1}{2}\left\{ \sum_{\vec{k}} \frac{\Delta_\gamma^2(\vec{k})}{E_\gamma^2(\vec{k})} th^2 \frac{E_\gamma(\vec{k})}{2\Theta} + \sum_{\vec{k}} {}^{\tau}\frac{\Delta_\tau^2(\vec{k})}{E_\tau^2(\vec{k})} th^2 \frac{E_\tau(\vec{k})}{2\Theta} \right\}. \tag{5}$$

Performing the integrations ($D, d > \Delta$) at zero temperature, one finds for $c < c_\beta$

$$n_{s0} = \frac{1}{2}\left\{ \Delta_\alpha \rho_\beta \mathrm{arctan}\frac{\beta c}{\Delta_\alpha} + \Delta_\gamma \rho_\gamma \mathrm{arccot}\frac{d_2 - \beta c}{\Delta_\gamma} \right\}, \tag{6}$$

and for $c > c_\beta < c_0$

$$\begin{aligned} n_{s0} = \frac{1}{2}\Big\{ \Delta_\alpha \rho_\beta \mathrm{arccot}\frac{d_2 - \beta c - \mu}{\Delta_\alpha} &+ \Delta_\alpha \rho_\alpha \mathrm{arccot}\frac{d_1 - \alpha c - \mu}{\Delta_\alpha} \\ &+ \Delta_\gamma \rho_\gamma \mathrm{arccot}\frac{\mu}{\Delta_\gamma} \Big\}. \end{aligned} \tag{7}$$

It can be seen that the presence of the normal state gap $d_2 - \beta c$ does not prepare a fermionic gap in the superfluid density. At the critical concentration $c = c_\beta$, n_s remains continuous (the second term in (7) tends to zero).

4. THE GAPS

Minimal quasiparticle energies reflect the presence of gaps in the excitation spectrum of the superconductor. This will be the case also for the pseudogaps, which appear naturally through the chosen normal state spectrum in the present

model. The basic source lies here in the perturbative segregation of the fermionic subsystem by the presence and localization of the doped holes.

In the low underdoped region for $c < c_\beta$ one has

$$E_\alpha(\min) = \Delta_l = \sqrt{(d_1 - \alpha c - \mu)^2 + \Delta_\alpha^2}, \tag{8}$$

$$E_\beta(\min) = \Delta_\alpha, \tag{9}$$

$$E_\gamma(\min) = \Delta_s = \sqrt{\mu^2 + \Delta_\gamma^2}. \tag{10}$$

Further, for $c > c_\beta$ and $c < c_0$, $E_\gamma(\min)$ will be represented by Δ_γ as $\xi_\gamma = \mu$ can be satisfied. For $c > c_0$ also $E_\alpha(\min)$ transforms into Δ_α.

In the normal state Δ_l and Δ_s survive and one interprets these as pseudogaps. A pseudogap and the corresponding normal state gap are connected through the contribution of $\Delta_{\alpha,\gamma}$ into E_σ. At $T = T_{\rm c}$, $\Delta_{\alpha,\gamma}$ vanish and the superconducting quasiparticle nature of the excitation is lost. In passing to the optimal doping the small pseudogap is smoothly transformed into the itinerant superconducting gap. The large pseudogap regime extends until $c \geq c_0$ is reached. The minimal excitation of the defect subsystem is further determined by the superconducting gap Δ_α. The connection and mutual transformation of the pseudogap and the corresponding superconducting gap are based on the doping-variable structure of the spectrum, which changes the nature of the minimal excitation energy of quasiparticles.

The opening of a pseudogap can be considered as a precursor of the superconducting gap opening, however, on the doping (not energetic) scale. It appears as "states nonconserving" (cf. [9]).

Concerning the manifestation of various gaps involved in the model, the valence band excitations belong to the "hot" spectrum. The "cold" spectrum is usually considered as nongapped [1–3,40]. If one accounts for the d-wave symmetry [40] by multiplying Δ_α with the corresponding symmetry function, the "cold" spectrum becomes empty. Note, however, that depending on the doping level and temperature, the two-band model allows for pure d-, s- or mixed d–s-ordering symmetries [46]. Extreme dopings and low temperatures favour the s-wave nature. In spite of that the basic gap manifestations appear in the "hot" spectrum and the "cold" electrons act essentially in building up the superconductivity high $T_{\rm c}$, supporting the interband pairing channel.

In summary, the present model allows the appearance of two pseudogaps on low dopings. Further the spectrum involves the large pseudogap and the itinerant superconducting gap. On overdoping the spectrum is expected to contain two superconducting gaps. Then the defect Δ_α will be manifested by an additional spectral weight inside Δ_γ. The superconductivity becomes spectrally exposed to a full extent on overdoping.

In the case where the β-subsystem states overlap the itinerant band from the very beginning, there will be only one defect subsystem pseudogap.

5. ILLUSTRATIONS AND COMPARATIVE DISCUSSION

The theoretical cuprate phase diagram following from the present model is illustrated by Figs. 1 and 2. The following plausible set of parameters has been used: $D = 2$, $d_1 = 0.3$ [47], $d_2 = 0.1$, $\alpha = 0.66$, $\beta = 0.33$, and $W = 0.28$ (eV), for which $T_{\rm c}(\max) = 125$ K is reached for $c = 0.57$, $c_\alpha = 0.45$, $c_\beta = 0.30$, and $c_0 = 0.57$. The scaling for a typical cuprate doping is made by $p = 0.28c$ according to the widely accepted value $p = 0.16$ corresponding to $T_{\rm c}(\max)$. The gaps in Fig. 1 are given for $T = 0$ and the connections between them can be followed on the doping scale. There seems to be a general agreement with the findings for cuprates.

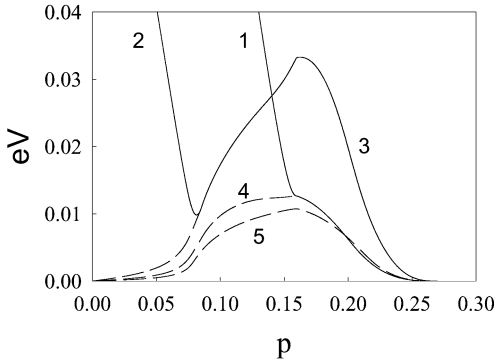

Fig. 1. Doping dependences of gaps: 1, the large pseudogap Δ_l; 2, the small pseudogap Δ_s; 3, the itinerant system superconducting gap Δ_γ; 4, the defect system superconducting gap Δ_α; 5, $T_{\rm c}$. $p = 0.28c$, $p_\alpha = 0.13$, $p_\beta = 0.085$, $p_0 = 0.16$, $p(T_{\rm c}(\max)) = 0.16$.

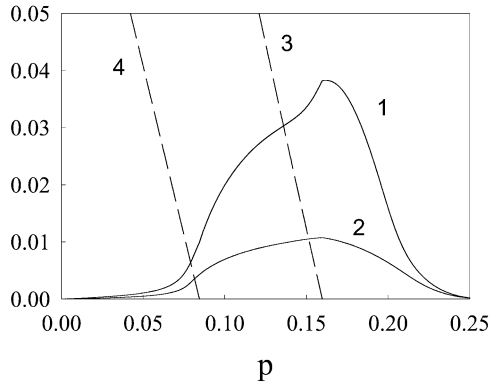

Fig. 2. Doping dependences of the superconducting density (curve 1) and of the transition temperature (curve 2). Curves 3 and 4 represent the normal state gaps. Energetic characteristics are given in eV.

The expected common manifestation of two underdoped state pseudogaps has been established for the La- and Bi-cuprates [5−7]. Another class of compounds with one charge channel pseudogap (bare nongapped β-subsystem) with the Δ_l-type behaviour is eventually possible. Smooth transformation of the small pseudogap into the larger superconducting gap (at p_β) has also been observed [5,6,13]. The large pseudogap extends to slight overdoping and then transforms into the defect system superconducting gap as found in [48]. The pseudogap Δ_l is attributed to the spectral hump-feature [9,10]. On intermediate dopings, Δ_l and the itinerant superconducting gap appear together. They cross close to the optimal doping. This corresponds to the observations of [9]. Note that in a narrow doping region the larger superconducting gap exceeds the pseudogap Δ_l. The corresponding parameters of the itinerant and defect subsystems are not competing. Eventually, the hump is shifted to larger energies with reduced dopings as observed in [10] and it is preserved for $T > T_{\rm c}$ on the dopings where $T_{\rm c}$ is optimized [9].

Following the connection of the pseudogap with its "own" subsystem superconducting gap, it can be seen that the manifestation of a superconducting gap on a given doping can be substituted by the appearance of the normal state gap (Fig. 2) for $T > T_{\rm c}$ in this region. It means that at low temperatures a pseudogap may not manifest itself on dopings where it will be found in the normal state (cf. [14]). In general, the pseudogaps persist to $T = 0$. The rising temperature expands slightly the region on the doping scale dawn where a pseudogap appears.

The manifestation of both superconducting gaps on overdoping is often debated. However, the Fermi energy intersects the electron spectrum parts headed by different band components at different wave vectors and the larger Δ_γ can remain masked.

The temperature dependence of the pseudogaps remains at the present state of the model due to the contribution of the superconducting gaps. This leads to a slow decrease in pseudogaps with $T \to T_{\rm c}$ [19], whereas the superconducting gaps $\Delta_{\alpha,\gamma}$ reach zero at $T_{\rm c}$ in a "traditional" manner [49] (cf. [48]). However, the formation of the reorganized spectrum by doping is projected on the phase separation into hole-rich and hole-poor regions. This process is expected to be influenced by temperature. Correspondingly a high-temperature limit for the formation of the bare gaps between itinerant and defect states can appear. This circumstance can limit the existence of the pseudogap phase.

Figure 2 represents the behaviour of the superconducting density ($T = 0$) together with the normal state gaps and $T_{\rm c}$. There are no signs of bare "extrinsic" fermionic gaps in a continuous trend of n_s and an argument [15] against the "extrinsic" source of the pseudogap fails. This is the result of the interband nature of the pairing. The normal state gaps and pseudogaps and their large ratios to $T_{\rm c}$ rise dramatically with the diminishing of doping, whereby the superconducting gaps and density decrease.

The behaviour of the superconducting density with the expressed maximum near the optimal doping follows the trends shown by $T_{\rm c}$ and superconducting

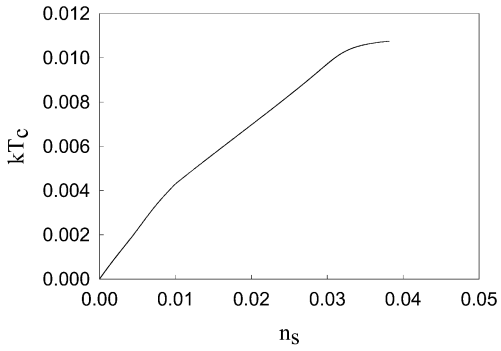

Fig. 3. Transition temperature vs. the superconducting density (the Uemura plot).

gaps. The strength of the pairing and the phase coherence develop and vanish simultaneously. This corresponds to recent experimental findings [$^{50-54}$].

In Fig. 3 the calculated Uemura-type [^{55}] plot is shown. On underdoping there is a sublinear segment connecting T_c and n_s with the further recession and turning back to zero.

The dynamics of the band overlap in the present model introduces a novel source for special critical dopings. These correspond to the doping concentrations where the band components begin to overlap. The metallization of the cold defect-liquid is reached at c_β. On smaller dopings the formation of doped hole ferrons and a percolation type superconductivity are supposed [^{56}]. The defect band acts as a bath of uncompensated spins. One can explain [^{37}] the presence of a magnetic pseudogap [^{57,58}] in the spin excitation channel on this basis.

The hot defect subsystem metallizes at c_0 near the optimal doping. Here all the three bands of the model overlap and are intersected by the chemical potential. This means that a common mixed Fermi liquid is formed. The difference between the defect and the itinerant carriers disappears. The large pseudogap gets lost when passing this border, where also n_s becomes maximal. Here one expects an insulator to metal transition in the normal phase. When this concentration is being achieved, the Fermi surface becomes more and more electron-like with peripheral hole pockets. Experiments on the normal phase [^{59}] show that a quantum metal to insulator transition appears at a distinct c_k in the same region where c_0 lies. For smaller dopings the hot quasiparticles become insulating where the cold quasiparticles remain metallic. Various experimental findings add to the existence of a critical doping concentration in cuprates [^{20,60,61}], where the properties of the electron liquid are essentially changed. Supposing that $c_k = c_0$, these findings become qualitatively explained. Such a c_k is of basic importance in a quantum critical point scenario [^{60}].

Some further essential properties of cuprates can be relatively simply explained by two-band models. The two observed electronic relaxation channels [^{48}] and coherence lengths are a natural property of two-band superconductors [^{62}].

The transition temperature and effective mass isotope effects can also be explained by two-band schemes [63,64]. In general, one observes a weak transition temperature effect for its optimal values and vice versa. This behaviour is caused by a contribution of a repulsive electron–phonon interaction in the whole pair-transfer scattering. This contribution of some percent in magnitude can cause the observed T_c-shifts. The pseudogap isotope effect [65] seems to be more complicated, being connected with the changes of both components in the quasiparticle energy.

The present simple model with plausibility elements seems to be able to reproduce qualitatively the behaviour of energetic characteristics of cuprate superconductors. There remains plenty of freedom to fill it in with better substantiated suppositions and quantitative aspects.

ACKNOWLEDGEMENT

This work was supported by the Estonian Science Foundation (grant No. 4961).

REFERENCES

1. Timusk, T. and Statt, B. The pseudogap in high-temperature superconductors: an experimental survey. *Rep. Progr. Phys.*, 1999, **62**, 61–122.
2. Timusk, T. The mysterious pseudogap in high temperature superconductors: an infrared view. *Solid State Commun.*, 2003, **127**, 337–348.
3. Damascelli, A., Hussain, Z. and Shen, Z.-X. Angle-resolved photoemission studies of the cuprate superconductors. *Rev. Mod. Phys.*, 2003, **75**, 473–541.
4. Mourachkine, A. Two energy gaps in cuprates: pairing and coherent gaps. The interpretation of tunneling and inelastic neutron scattering measurements. *Physica C*, 2000, **341–348**, 917–918.
5. Dipasupil, R. M., Oda, M., Momono, N. and Ido, M. Energy gap evolution in the tunneling spectra of $Bi_2Sr_2CaCu_2O_{8+\delta}$. *J. Phys. Soc. Jpn.*, 2002, **71**, 1535–1540.
6. Sato, T., Naitoh, Y., Kamiyama, T., Takahashi, T., Yokoya, T., Yamada, K., Endoh, Y. and Kadowaki, K. Small and large pseudogaps in high-T_c superconductors observed by ultrahigh-resolution photoemission spectroscopy. *Physica C*, 2000, **341–348**, 815–818.
7. Fujimori, A., Ino, A., Yoshida, T., Mizokawa, T., Nakamura, M., Kim, C., Shen, Z.-X., Kakeshita, T., Eisaki, H. and Uchida, S. Fermi surface, pseudogap and superconducting gap in $La_{2-x}Sr_xCuO_4$. *Physica C*, 2000, **341–348**, 2067–2070.
8. Takahashi, T., Sato, T., Yokoya, T., Kamiyama, T., Naitoh, Y., Mochiku, T., Yamada, K., Endoh, Y. and Kadowaki, K. Two different types of pseudogaps in high-T_c superconductors. *J. Phys. Chem. Solids*, 2001, **62**, 41–45.
9. Krasnov, V. M., Yurgens, A., Winkler, D., Delsing, P. and Claeson, T. Evidence for coexistence of the superconducting gap and the pseudogap. *Phys. Rev. Lett.*, 2000, **84**, 5860–5863.
10. Miyakawa, N., Zasadzinski, J. F., Ozyuzer, Y., Guptasarna, P., Hinks, P. G., Kendziora, C. and Gray, K. F. Predominantly superconductive origin of large energy gaps in underdoped $Bi_2Sr_2CaCu_2O_{8+\delta}$. *Phys. Rev. Lett.*, 1999, **83**, 1018–1021.
11. Tallon, J. L. and Loram, J. W. The doping dependence of T^* – what is the real high-T_c phase diagram? *Physica C*, 2001, **349**, 53–68.

12. Moraghebi, M., Buhler, C., Yunoki, S. and Moreo, A. Fermi surface and special functions of hole-doped spin-fermion model for cuprates. *Phys. Rev. B*, 2001, **63**, 214513-10.
13. Ino, A., Kim, C., Nakamura, M., Yoshida, T., Mizokawa, W., Fujimori, A., Shen, Z.-Y., Kakeshita, T., Eisaki, H. and Uchida, S. Doping-dependent evolution of the electronic structure of $La_{2-x}Sr_xCuO_4$ in the superconducting and metallic phases. *Phys. Rev. B*, 2002, **65**, 094504-11.
14. Ozyuzer, Y., Zasadzinski, J. F., Gray, K. E., Kendziora, C. and Miyakawa, N. Absence of pseudogap in heavily overdoped $Bi_2Sr_2CaCuO_2O_{8+\delta}$. *Europhys. Lett.*, 2002, **58**, 589–595.
15. Stajic, J., Yvengar, A., Levin, K., Boyce, B. R. and Lemberger, T. R. Cuprate pseudogap: competing order parameters or precursor superconductivity. *Phys. Rev. B*, 2003, **68**, 024520-9.
16. Müller, K. A. Recent experimental insights into HTSC materials. *Physica C*, 2000, **341–348**, 11–18.
17. Bianconi, A. and Saini, N. (eds.). *Stripes and Related Phenomena*. Kluwer Academic Publishers, N-Y, 2000.
18. Kristoffel, N. and Rubin, P. Two-band high-T_c superconductivity with a pseudogap. *Physica C*, 2001, **356**, 171–175.
19. Kristoffel, N. and Rubin, P. Cuprate superconductivity interband model with doping formed spectrum. *Eur. Phys. J. B*, 2002, **30**, 495–500.
20. Schwaller, P., Greber, T., Aebi, T., Singer, J. M., Berger, H., Forro, L. and Osterwalder, J. Doping-dependent electronic structure of cuprates studied using angle scanned photoemission. *Eur. Phys. J. B*, 2000, **18**, 215–225.
21. Ando, Y., Lavrov, A. N., Komiya, S., Segawa, K. and Sun, X.-F. Mobility of the doped holes and the antiferromagnetic correlations in underdoped high-T_c cuprates. *Phys. Rev. Lett.*, 2001, **87**, 017001-4.
22. Homes, C. C., Tranquada, J. M., Li, Q., Moodenbaugh, A. R. and Buttray, D. J. Mid-infrared conductivity from mid-gap states associated with charge stripes. *Phys. Rev. B*, 2003, **67**, 184516-7.
23. Borisov, A. A., Gavrichkov, V. A. and Ovchinnikov, S. G. Doping dependence of the band structure and chemical potential in cuprates. *Modern Phys. Lett.*, 2003, **17**, 479–486.
24. Emery, V. J. and Kivelson, S. A. Frustrated electronic phase separation and high-T_c superconductors. *Physica C*, 1993, **219**, 597–621.
25. Tranquada, J. Stripe correlations of spins and holes in cuprate superconductors. *J. Supercond.*, 1996, **9**, 397–399.
26. Bianconi, A., Valletta, A., Perali, A. and Saini, N. L. Superconductivity of a striped phase at the atomic limit. *Physica C*, 1998, **296**, 269–280.
27. Phillips, J. C. and Jung, J. Nanodomain structure and function of high-temperature superconductors. *Phil. Mag. B*, 2001, **81**, 745–756.
28. Kristoffel, N. and Rubin, P. Pseudogap and superconductivity gaps in a two-band model with doping determined components. *Solid State Commun.*, 2002, **122**, 265–268.
29. Kristoffel, N. and Rubin, P. Cuprate superconductivity on interacting electronic components prepared by doping. *Int. J. Modern Phys. B*, 2002, **16**, 1739–1742.
30. Kristoffel, N. and Rubin, P. Superconducting gaps and pseudogaps in a composite model of two-component cuprate. *Physica C*, 2004, **402**, 257–262.
31. Suhl, H., Matthias, B. T. and Walker, L. R. Bardeen–Cooper–Schriffer theory of superconductivity in the case of overlapping bands. *Phys. Rev. Lett.*, 1959, **3**, 552–554.
32. Moskalenko, V. A. Superconductivity for overlapping electron bands. *Fiz. Met. i Metalloved.*, 1959, **8**, 503–510.
33. Kristoffel, N., Konsin, P. and Örd, T. Two-band model for high-temperature superconductivity. *Riv. Nuovo Cimento*, 1994, **17**, 1–41.

34. Gorkov, L. P. and Sokol, A. V. Phase separation of electronic liquid in novel superconductors. *Pis'ma ZETF*, 1987, **46**, 333–336.
35. Bussmann-Holder, A., Müller, K. A., Micknas, R., Büttner, H., Simon, A., Bishop, A. R. and Egami, T. Theory of dynamic stripe induced superconductivity. *J. Phys.: Cond. Matter*, 2001, **13**, L169–L174.
36. Perali, A., Castellani, C., Di Castro, C., Grilli, N., Piegari, E. and Varlamov, A. A. Two-gap model for underdoped cuprate superconductors. *Phys. Rev. B*, 2000, **62**, R9295–R9298.
37. Alexandrov, A. S. and Edwards, P. P. High-$T_{\rm c}$ cuprates: a new electronic state of matter? *Physica C*, 2000, **331**, 97–112.
38. Micknas, R., Robaszkiewicz, S. and Bussmann-Holder, A. On the superconductivity in the induced pairing model. *Physica C*, 2003, **387**, 58–64.
39. Kristoffel, N. Description of two-component high-$T_{\rm c}$ superconductors by an interband model. *phys. stat. sol. b*, 1998, **210**, 195–198.
40. Tsuei, C. C. and Kirtley, J. Pairing symmetry in cuprate superconductors. *Rev. Mod. Phys.*, 2000, **72**, 969–1016.
41. Zhao, G., Li, E., Wu, T., Ogale, S. B., Sharma, R. P., Venkatesan, T., Li, J. J., Cao, W. L., Lee, C. H., Sato, H., and Naito, M. Optical Cooper pair breaking spectroscopy of cuprate superconductors. *Phys. Rev. B*, 2001, **63**, 132507-4.
42. Calvani, P. Large polaron absorption in high-$T_{\rm c}$ cuprates. *phys. stat. sol. b*, 2003, **237**, 194–203.
43. Gromko, A. D., Fedorov, A. V., Chuang, Y., Koralek, J. D., Aiura, Y., Yamaguchi, Y., Oka, K., Ando, Y. and Dessau, D. S. Mass-renormalized electronic excitations at $(\pi, 0)$ in the superconducting state. *Phys. Rev. B*, 2003, **68**, 174520-7.
44. Sugai, S., Suzuki, H., Takayanagi, Y., Hosakawa, T. and Hayamizu, N. Carrier-density-dependent momentum shift of the coherent peak in p-type high-$T_{\rm c}$ superconductors. *Phys. Rev. B*, 2003, **68**, 184504-19.
45. Markiewicz, R. S. A survey of the van Hove scenario for high-$T_{\rm c}$ superconductivity. *J. Phys. Chem. Solids*, 1997, **58**, 1179–1310.
46. Konsin, P., Kristoffel, N. and Rubin, P. S+D symmetry order parameters in interband superconductivity. *phys. stat. sol. b*, 1998, **208**, 145–150.
47. Boris, A. V., Kovaleva, N. N., Dolgov, D. V., Holden, T., Liu, C., Keimer, B. and Bernhard, C. In-plane spectral weight shift of charge carrier in $YBa_2Cu_3O_{6.9}$. *Science*, 2004, **304**, 708–710.
48. Mihailovic, D., Demsar, J., Hudej, R., Kabanov, V. V., Wolf, T. and Karpinski, J. Quasiparticle relaxation dynamics in cuprates. *Physica C*, 2000, **341–348**, 1731–1734.
49. Konsin, P., Kristoffel, N. and Rubin, P. Dependences of superconducting gaps on temperature and carrier concentration in a two-band model. *Solid State Commun.*, 1996, **97**, 567–572.
50. Feng, D. L., Lu, D. H., Shen, K. M., Kim, C., Eisaki, H., Damascelli, A., Yashizaki, R., Shimoyama, J., Kishio, K., Gu, G., Oh, S., Andrus, A., O'Donnel, J., Eckstein, J. and Shen, Z.-H. Signature of superfluid density in the single particle excitation spectrum of $Bi_2Sr_2CaCu_2O_{8+\delta}$. *Science*, 2000, **289**, 277–281.
51. Trunin, M. R., Nefyodov, Yu. A. and Shevchuk, A. F. Superfluid density in the underdoped $YBa_2Cu_3O_{7-x}$ *Phys. Rev. Lett.*, 2004, **92**, 067006-4.
52. Tallon, J. L., Loram, J. W., Cooper, J. R., Panagopoulos, C. and Bernhard, C. Superfluid density in cuprate high-$T_{\rm c}$ superconductors: a new paradigm. *Phys. Rev. B*, 2003, **68**, 180501-4(R).
53. Schneider, T. Universal properties of cuprate superconductors. *Physica B*, 2003, **326**, 283–295.

54. Bernhard, C., Tallon, J. L., Blasius, Th., Golnik, A. and Niedermayer, Ch. Anomalous peak in the superconducting condensate density of cuprate high-T_c superconductors. *Phys. Rev. Lett.*, 2001, **86**, 1614–1617.
55. Uemura, Y. J. Energy scales of exotic superconductors. In *Polarons and Bipolarons in High-T_c Superconductors and Related Materials* (Salje, E. K. H., Alexandrov, A. S. and Liang, W. Y., eds.). Cambridge University Press, 1995, 453–460.
56. Hizhnyakov, V., Kristoffel, N. and Sigmund, E. On the percolation induced conductivity in high-T_c superconducting materials. *Physica C*, 1989, **161**, 435–440.
57. Kitazawa, K. Physical properties of the high-temperature superconductors. *Physica C*, 2000, **341–348**, 19–24.
58. Deutcher, G. Coherence and single particle excitations in high-T_c superconductors. *Nature*, 1999, **397**, 410–412.
59. Venturini, F., Opel, M., Devereaux, T. P., Freericks, J. K., Tüttö, T., Revaz, B., Walker, E., Berger, H., Forro, L. and Hackl, R. Observation of an unconventional metal-insulator transition in overdoped CuO_2 compounds. *Phys. Rev. Lett.*, 2002, **89**, 107003-4.
60. Di Castro, D., Bianconi, G., Colapietro, M., Pifferi, A., Saini, N. L., Agrestini, S. and Bianconi, A. Evidence for the strain critical point in high-T_c superconductors. *Eur. Phys. J. B*, 2000, **18**, 617–624.
61. Liang, W. Y. Are high-T_c cuprates unusual metals? *J. Phys. Cond. Matter*, 1998, **10**, 11365–11384.
62. Örd, T. and Kristoffel, N. Two relaxation times and the high-T_c superconductivity two-component scenario. *Physica C*, 2000, **331**, 13–17.
63. Konsin, P., Kristoffel, N. and Örd, T. On the composition dependent isotope effect of HTSC in the two-band model. *Ann. Physik*, 1993, **2**, 279–283.
64. Örd, T. and Kristoffel, N. Paired carrier effective mass isotope effect in the two-band model. *phys. stat. sol. b*, 1999, **216**, 1049–1056.
65. Temprano, D., Mesot, J., Janssen, S., Conder, K., Furrer, A., Mutka, H. and Müller, K. A. Large isotope effect on the pseudogap in high-T_c superconductor $HgBa_2Cu_4O_8$. *Phys. Rev. Lett.*, 2000, **84**, 1990–1993.

Kahekomponendiline stsenaarium, kupraatide seotud pilud ja ülijuhtivustihedus

Nikolai Kristoffel ja Pavel Rubin

On esitatud lihtne mudel kupraatide ülijuhtivuse kirjeldamiseks. On kasutatud dopeerimisega kujundatud elektronspektrit. Paariülekande tüüpi interaktsioon toimib valentstsooni ja defektsüsteemi komponentide (“kuum” ja “külm”) vahel. Lähtepilud põhiaine ja defektsüsteemi vahel sulguvad dopeerimise kasvuga. Tsoonide kattumine osutub uudseks kriitiliste dopeerimiskontsentratsioonide alliikaks. Kvaasiosakeste minimaalsed energiad määratlevad ülijuhtivus- ja pseudopilud vastavalt tsoonide dopeerimisest sõltuvale asendile. Seosed pilude, pseudopilude ja normaalseisundi pilude vahel faasidiagrammil on kooskõlas mitmetahuliste uurimistulemustega. Ülijuhtivustihedus ei peegelda “väliste” lähtepilude olemasolu paardumise tsoonidevahelise iseloomu tõttu. On saadud sublineaarne Uemura-tüüpi sõltuvus aladopeeritud piirkonnas. Fermivedelikuline käitumine taastub optimaalsel dopeeringul, kus keemiline potentsiaal lõikub kolme kattuva tsooniga.